Vol. 16, No. 2 (2017) 663-678

Simulación y Control

Revista Mexicana de Ingeniería Química

DESARROLLO DE UN SISTEMA DE CONTROL DIFUSO PARA UN CRISTALIDOR CONTINUO NO ISOTÉRMICO

DEVELOPMENT OF A FUZZY CONTROL SYSTEM FOR A NON-ISOTHERMAL CONTINUOUS CRYSTALLIZER

P. A. Quintana-Hernández[1,*], C. G. Aguilar-Madera[1], S. Tututi-Ávila[1] and L.I. Salcedo-Estrada[2].

[1] *Departamento de Ingeniería Química. Instituto Tecnológico de Celaya. Av. Tecnológico y García Cubas s/n. 38010 Celaya, Guanajuato, México.*

[2] *Facultad de Ingeniería Química. Universidad Michoacana de San Nicolás de Hidalgo. Ciudad Universitaria. 58060 Morelia, Michoacán, México.*

Recibido 19 de Septiembre de 2016; Aceptado 4 de Abril de 2017

Resumen

Se desarrolló un algoritmo de control difuso de múltiples entradas-múltiples salidas (MIMO) para controlar un cristalizador continuo no isotérmico. El algoritmo incluye dos lazos de control por retroalimentación y dos desacopladores. El primer lazo controla la temperatura del cristalizador manipulando el flujo de agua de refrigeración, y el segundo lazo controla la media de la distribución de tamaño de cristales mediante la manipulación de la velocidad de agitación. Tanto los controladores como desacopladores difusos fueron entrenados usando información generada a través de simulaciones a lazo abierto. El algoritmo difuso se comparó contra un sistema MIMO con controladores PID convencionales usando la medición de la integral del cuadrado del error (ICE) y la integral el valor absoluto del error (IAE) ante cambios en el punto de ajuste en la temperatura del cristalizador y en la media de la distribución del tamaño de cristal. También se analizaron los efectos de las perturbaciones provocados por cambios en la temperatura del líquido refrigerante. Los controladores fueron sintonizados minimizando la ICE usando el algoritmo de ajuste de mínimos cuadrados no lineales de Matlab (lsqnonlin). Los resultados mostraron que el algoritmo de control difuso podía ser utilizado con éxito para controlar la operación de un cristalizador continuo no isotérmico.

Palabras clave: control difuso, control MIMO, cristalización, desacopladores difusos, modelado.

Abstract

A fuzzy multiple-input-multiple-output (MIMO) control algorithm was developed and applied to control a non-isothermal continuous crystallizer. The algorithm included two feedback control loops and two decouplers. The first loop controls the crystallizer temperature manipulating the cooling water flow rate, and the second loop controls the crystal size distribution mean manipulating the agitation rate. Fuzzy controllers and decouplers were trained using open loop simulated information. The fuzzy algorithm was compared to a MIMO conventional PID control system measuring the integral of square error (ISE) and the integral of the absolute value error (IAE) when temperature and crystal size distribution mean set points changed. In addition, disturbances caused by changes in the cooling water temperature were analyzed. Fuzzy and conventional controllers were tuned by minimizing the ISE using the nonlinear least-squares Matlab algorithm (lsqnonlin). The results showed that the fuzzy control algorithm could be successfully used to control a non-isothermal continuous crystallizer.

Keywords: crystallization, fuzzy control, fuzzy decoupling, MIMO control, modeling.

1 Introduction

The crystallization process is an old separation method currently used for obtaining high-value commodities in batch processes, or large-volume products in continuous processes. At industrial level, the main objective of crystallization is to obtain solid products with a specified quality and suitable conditions for packaging and storage. These conditions can be achieved when good control strategies are applied and control objectives are attained. Different control strategies have been

developed for isothermal continuous crystallization (Lakatos, *et al*., 2007; Pathath and Kienle, 2003; Bravi and Chianese, 2003); however, continuous non-isothermal crystallization has not been widely analyzed due to lack of precise information concerning the metastable zone width and kinetic parameters for nucleation and growth. Quintana *et al*., (2005) reported the evaluation of kinetic parameters of sugar cane and a novel technique for evaluating the metastable zone with for adipic acid (Quintana *et al*., 2016). On the other hand, Quintana *et al*., (2012) developed a nonlinear feedback controller using geometric control theory for a non-isothermal crystallizer. They found that interactions among non-linear parameters introduced a cycling behavior that easily lead to an unstable operation and the process was difficult to control when it had an intrinsic unstable behavior with time-varying parameters. Other strategy for controlling non-isothermal continuous crystallizer was reported by Zempoaltécatl (2006). He used Model Predictive Control with information for the ammonium sulfate-water system.

On the other hand, fuzzy control algorithms have been successfully applied to control mechanical systems (Chebolu, 2004; Shelare, 2004; Gupta, 2005; Thompson and Dexter, 2005; Odetunji and Kehinde, 2005; Andújar and Bravo, 2005; Park and Cho, 2005; Kocaarslan *et al*., 2006). Zhang and Feng (1997) used fuzzy logic to design a decentralized adaptive control for large-scale nonlinear systems; Li and Priemer (1999) and Shaocheng *et al*., (2005) controlled a multiple-input-multiple-output (MIMO) plant. Similarly, Kim and Oh (2000) utilized fuzzy logic to control nonlinear and uncertain systems; Lian and Huang (2001) used fuzzy algorithms for controlling and decoupling a MIMO plant simultaneously according to the dynamics system characteristics; and Chen and Chang (2006) developed a fuzzy diagnosis method to control systems with coupled loops. Particularly in crystallization processes, Bravi and Chianese (2003) developed a neuro-fuzzy controller to control a continuous cooled mixed-suspension-mixed-product-removal (MSMPR) potassium sulfate crystallizer. The control system kept the operation in stable regions and presented short transient responses. Tututi-Ávila (2007) applied fuzzy inference to control isothermal and non-isothermal continuous ammonium sulfate crystallizers. He reported better performance when compared to traditional PID controllers but only in narrow operation ranges due to the interactions between the control variables. In this work, a fuzzy control strategy with fuzzy decouplers is developed to control a non-isothermal ammonium sulfate crystallizer, and its performance is compared to conventional PID control systems.

2 Crystallization process model

The crystallization process model includes mass, energy and population balances. The mass balance considers the solute concentration in the continuous phase and accounts for flow of solute into and out of the system and mass transfer to the solid phase (nucleation and growth of crystals). In the same way, the energy balance considers the enthalpy differences between the flow streams, the heat of crystallization and heat removal by the cooling system. The population balance uses the concept of particle size distribution to include an arbitrary number of internal coordinates necessary to describe the state of the particles. The overall model is developed under the following considerations: continuous operation, perfect mixing, infinitesimal generated particles and constant volume. The population balance is reduced to a five differential equations using the method of moments and assuming that the dominant dynamic of the system may be represented by a small number of degrees of freedom. The complete model is represented by eqs. (1)-(5).

$$\frac{dM_0}{dt} = \frac{M_{0,feed} - M_0}{\tau} + B \tag{1}$$

$$\frac{dM_j}{dt} = \frac{M_{j,feed} - M_j}{\tau} + GjM_{j-1} \quad j = 1,...,4 \tag{2}$$

$$\frac{dC}{dt} = \frac{(\varepsilon C)_{feed}C + M_{3,feed}C - 3\tau GM_2(\rho_c - C)}{\tau(1 - M_3)} \tag{3}$$

$$\frac{dT}{dt} = \frac{\rho f C_p(T_{feed} - T) - 3\Delta H_c \rho_c k_v VGM_2 - UA(T - T_c)}{\rho V C_p} \tag{4}$$

$$\frac{dT_c}{dt} = \frac{\rho_w F_w C_{pw}(T_{c,feed} - T_c) + UA(T - T_c) - (UA)_\infty (T_c - T_\infty)}{\rho_w V_c C_{pw}} \tag{5}$$

The nucleation (B) and growth (G) parameters are calculated on the basis of the solution concentration and agitation rate. Salcedo-Estrada (2000) evaluated these parameters into the metastable crystallization using Eqs. (6)-(7). Table 1 includes the values for all the involved physical constants and operation conditions for solving the mathematical model.

$$B = k_b S_r^b M_t^o N_r^p \tag{6}$$

$$G = k_g S_r^g N_r^h \tag{7}$$

Eqs. (8)-(9) limit the metastable zone width for the ammonium sulfate water system. The first one represents the saturation equation and it was reported by Perry *et al*., (1992). The second one represents the limit of the metastable zone width, and it was reported by Lugo (2005).

Table 1. Physics constants and operation values.

Parameter	Value
b	0.562
g	1.5
h	1.337
k_b	180
k_g	9.09×10^{-4}
k_v	0.99
o	0.001
p	0.05
C_{feed}	0.763
C_p	0.6816
C_{pw}	1
T_{feed}	25
$T_{c,feed}$	5
T_∞	29
$M_{43,feed}$	170
UA	400
$(UA)_x$	100
V	2230
V_c	820
ε	0.98
ρ	1.244
ρ	1.769
ρ	1
ΔH_v	−12.0354
τ	2.6

$$C_s = 4 \times 10^{-5} T^2 + 2 \times 10^{-4} T + 0.73 \tag{8}$$

$$C_l = 1.3179 \times 10^{-7} T^3 + 2.6136 \times 10^{-6} T^2 + 2.6280 \times 10^{-3} T + 0.7076 \tag{9}$$

3 Design of the fuzzy control system

Fig. 1 presents the proposed fuzzy control scheme. The fuzzy controller 1 (FC1) controls the crystal size distribution mean (evaluated as the ratio of moment 4 and moment 3) manipulating the stirring rate, and fuzzy controller 2 (FC2) controls the crystallizer temperature manipulating the cooling water flow rate. The pairing of these variables was made based on the relative gains array analysis performed by Tututi-Ávila (2007). The fuzzy decoupler 1 (FD1) minimizes the interaction between the FC1control action and temperature; and the fuzzy decoupler 2 (FD2) minimizes the interaction between the FC2 control action and the crystal size distribution mean.

3.1 Design of FC1 and FC2

Fuzzy controllers were developed on a PID fuzzy structure given by Eq. (10) and shown schematically in Fig. 2. The error and its derivative constitute the input variable and the control action represents the output variable. Three levels for error and its derivative were considered (negative, zero and positive) and their combinations generate five possible values for the output variable (big negative, small negative, zero, small positive and big positive). These values were used to build the inference rules. The training routine ANFIS (Adaptive-Network-based Fuzzy Inference Systems) of Matlab was used for the fuzzy fit process. ANFIS routine uses a hybrid learning algorithm to identify fuzzy inference systems with Sugeno-type parameters, and it applies a combination of the least-squares method and the back propagation gradient descent method.

Table 2. Design parameters of the fuzzy inference engines of FC1 and FC2.

PARAMETER	**FUZZY INFERENCE ENGINE**	
	PD-FC1 and PI-FC1	**PD-FC2 and PI-FC2**
Type	*Sugeno*	*Sugeno*
And method	*product*	*product*
Or method	*probor*	*probor*
Defuzzyfication method	*weight average*	*weight average*
Aggregate method	*sum*	*sum*
Implication method	*product*	*product*
Inputs (2)	*e, de/dt*	*e, de/dt*
Outputs (1)	*Nr*	*Fw*
Inputs range	[-100,100],[-100,100]	[-5,5], [-100,100]
Inputs membership	e: neg, zero, pos	e: neg, zero, pos
Functions labels	de/dt: neg, zero, pos	de/dt: neg, zero, pos
Outputs membership	Nr: bn, sn, z, sp, bp	Fw: bn, sn, z, sp, bp
Inputs membership	*gauss*	*gauss*
Functions types	*It distributes on all range*	*It distributes on all range*
Outputs membership	*constants:*	*constants:*
Functions types	-100, -50, 0, 50, 100	-2000, -1000, 0, 1000, 2000
Base rules	If pos and pos then bp If pos and zero then sp If pos and neg then zero If zero and pos then sp If zero and zero then zero If zero and neg then sn If neg and pos then zero If neg and zero then sn If neg and neg then bn	If pos and pos then bn If pos and zero then sn If pos and neg then zero If zero and pos then sn If zero and zero then zero If zero and neg then sp If neg and pos then zero If neg and zero then sp If neg and neg then bp

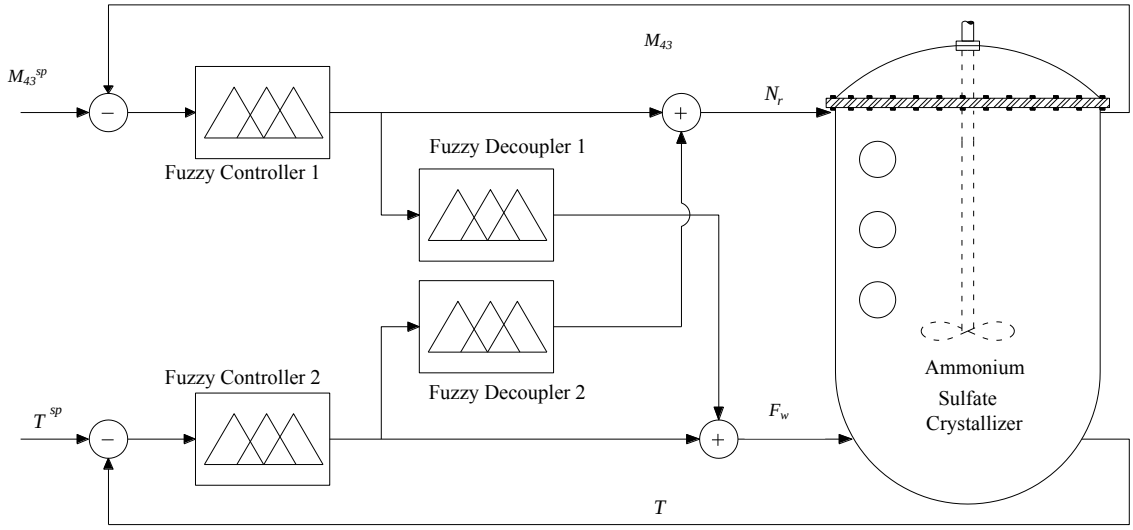

Fig. 1. Proposed control scheme.

$$u(t) = \int \left\{ \frac{FK_c}{2} \frac{d[e(t)]}{dt} + FK_i e(t) \right\} + \frac{FK_c}{2} e(t) + FK_d \frac{d[e(t)]}{dt} \tag{10}$$

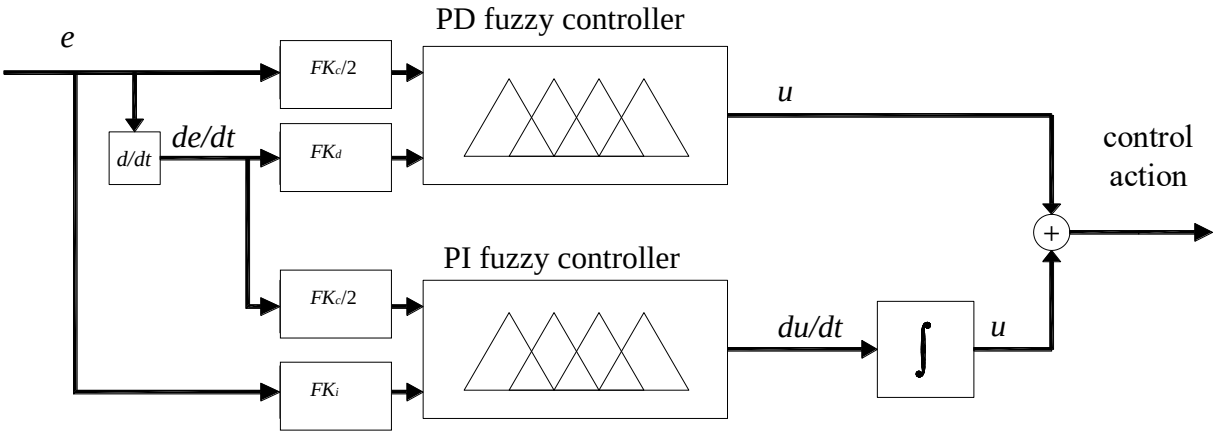

Fig. 2. Scheme of the fuzzy controller.

Each fuzzy block in Fig. 2 represents a fuzzy inference engine. The design parameters required to run the ANFIS routine for the inference engines are shown in table 2. The selected ranges for the error and its derivative go from -100 to 100 except for the error in the FC2 because the final control element in the temperature-water flow rate loop has less sensitivity and only allows ten defined valve stem positions. The range for the associated error goes from -5 to 5. On the other hand, the outputs membership functions types are defined on the basis of the nominal upper and lower operation values for F_w (10000, 100) and N_r (600,100). The selected values represent forty percent of the nominal range F_w (-2000, 2000) and Nr (100, -100). No differences were found on the final process control responses when the ranges were F_w (-5000, 5000) and N_r (-250, 250) but larger computational times. Fig. 3 shows the calculated values for the manipulated variables as function of the error and its derivative in the defined output ranges. Big positive errors in the FC1 are associated with large control actions as well as big negative errors in the FC2.

3.2 Design of FD1 and FD2

Eqs. (11)-(12) represent the open-loop total derivate of the controlled variable used for designing the fuzzy decouplers.

$$\frac{dM_{43}}{dt} = \frac{dN_r}{dt}\left(\frac{\partial M_{43}}{\partial N_r}\right)_{F_w} + \frac{dF_w}{dt}\left(\frac{\partial M_{43}}{\partial F_w}\right)_{N_r} \tag{11}$$

$$\frac{dT}{dt} = \frac{dN_r}{dt}\left(\frac{\partial T}{\partial N_r}\right)_{F_w} + \frac{dF_w}{dt}\left(\frac{\partial T}{\partial F_w}\right)_{N_r} \tag{12}$$

In order to keep the desired controlled variables constant under any change in the manipulated variables the left hand side of eqs. (11)-(12) has to be equal to zero, and the decoupling actions may be evaluated from eqs. (11)-(12). FD1 (N_r-T) loop is obtained from eq. 11 and FD2 (F_w-M_{43}) from eq. 12. The decoupling control actions are represented by eqs. (13)-(14).

$$\frac{dF_w}{dt} = -1\frac{dN_r}{dt}\left(\frac{\partial T}{\partial N_r}\right)_{F_w}\left(\frac{\partial F_w}{\partial T}\right)_{N_r} \tag{13}$$

$$\frac{dN_r}{dt} = -1\frac{dF_w}{dt}\left(\frac{\partial M_{43}}{\partial F_w}\right)_{N_r}\left(\frac{\partial N_r}{\partial M_{43}}\right)_{F_w} \tag{14}$$

Table 3. Design characteristics of the fuzzy inference engines for $\partial T/\partial N_r$, $\partial N_r/\partial M_{43}$, $\partial F_w/\partial T$ and $\partial M_{43}/\partial F_w$.

Parameter	Value
Type	*Sugeno*
And method	*product*
Or method	*probor*
Defuzzyfication method	*weight average*
Aggregate method	*sum*
Implication method	*product*
Inputs	2: N_r, F_w
Outputs	1: Output
Inputs range	[100,600], [100,10000]
Inputs membership functions labels	N_r: N_1, N_2, N_3 F_w: f_1, f_2, f_3
Outputs membership functions labels and types	Output: O_1,...,O_9 type: all constants
Inputs membership functions types	*gauss* It distributes on all range
Base rules	If N_i and f_i then O_{3i+j-3} $i = 1,2,3$ $j = 1,2,3$

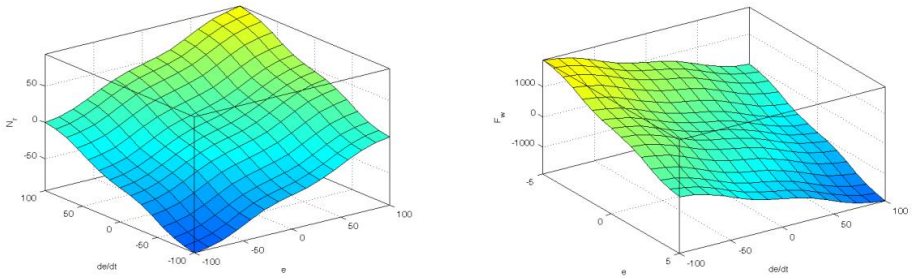

(a) (b)

Fig. 3. Control actions for a) FC1 and b) FC2 as function of error and its derivative.

The derivative terms in eqs. (13)-(14) represent on-line signals, while the partial derivative terms represent uncertainties of the plant dynamics. Partial derivatives were represented by fuzzy structures and evaluated by open loop simulation using known values for the manipulated variables. Fig. 4 shows the scheme used to generate the information needed for the inference engine. The K weight parameters include the minus sign of eqs. (13)-(14). A Gaussian type scheme with three membership function associated with the input variable and zero order (constant) associated with the output variable was used to train the fuzzy decouplers. Table 3 shows the design parameters for the fuzzy inference engines, and Tables 4-7 show the obtained simulated values for the partial derivative terms. Fig. 5 shows the surface response for each partial derivative term.

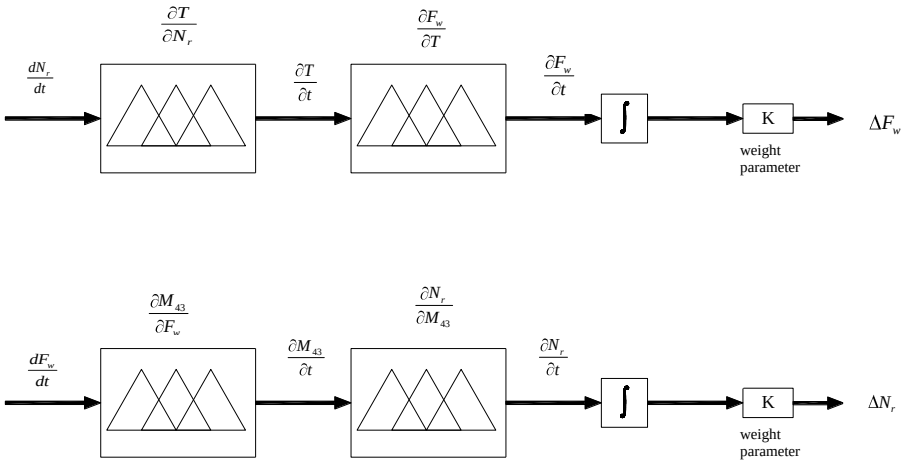

Fig. 4. Scheme of fuzzy decouplers.

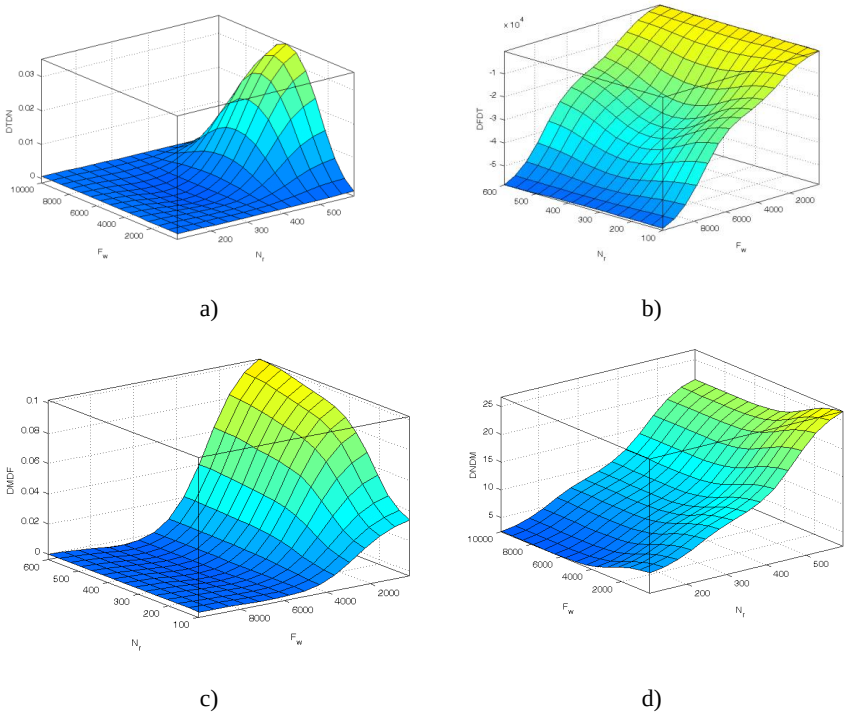

Fig. 5. Control fit surfaces of partial derivatives: a) $(\partial T/\partial N_r)_{F_w} = DTDN$, b) $(\partial F_w/\partial T)_{N_r} = DFDT$, c) $(\partial M_{43}/\partial F_w)_{N_r} = DMDF$ and d) $(\partial N_r/\partial M_{43})_{F_w} = DNDM$.

4 Design of the conventional PID control system

Tututi-Ávila (2007) developed a conventional PID system (CC1 for the M43-Nr loop and CC2 for the T-Fw loop) for controlling the operation of a non isothermal crystallizer. He used the crystallization model previously described to adjusted process reaction curves to a first order plus dead time models for each control loop and second order models for decouplers. Eqs. (15)-(16) show the relationship between the controlled variables and manipulated variables, and eqs. (17)-(18) show the transfer functions for decouplers.

$$G_{M_{43},N_r}(s) = \frac{0.2285e^{-1.117s}}{3.6246s+1} \tag{15}$$

$$G_{T,F_r}(s) = \frac{-7.5982\times10^{-4}e^{-0.5716s}}{1.805s+1} \tag{16}$$

$$D_{M_{43},F_w} = -0.1099\left(\frac{4.8841s^2+4.42s+1}{13.235s^2+7.276s+1}\right) \tag{17}$$

$$D_{T,N_r} = 0.3177\left(\frac{1.2746s^2+2.258s+1}{0.1105s^2+0.645s+1}\right) \tag{18}$$

Table 4. Simulated partial derivatives values $(\partial T/\partial N_r)_{F_w}$ for known F_w and N_r values.

	N_r, **rpm**		
F_w, (ml/min)	**105**	**355**	**595**
100	3.40×10^{-4}	1.40×10^{-4}	1.02×10^{-4}
5000	5.94×10^{-4}	1.83×10^{-4}	3.52×10^{-2}
10000	6.18×10^{-4}	2.25×10^{-4}	5.24×10^{-5}

5 Results

The evaluation of the servo control for both fuzzy and conventional control schemes was made changing the set point of the controlled variables. The conventional PID control scheme had the same elements as the fuzzy control scheme (two control loops and two control decouplers). Five cases were analyzed in this work. In the first one, crystal size distribution mean was changed from 170 μm to 187 μm and crystallizer operation temperature from 25 °C to 23 °C. In the second case, set point changes were broadened (170-210 μm and 25-21 °C). In the third case, crystal size distribution mean set point was change every 25 minutes (170-187-195-178 μm). In the fourth case, crystallizer temperature set point was changed every 25 minutes (25-23-22-23 °C) and in the fifth case, disturbance in the cooling water temperature were introduced at times 25 and 50 minutes (5-15-5 °C).

Controllers were tuned (six parameters) at the same time minimizing the sum of the integral square errors using the lsqnonlin Matlab algorithm. The optimization process was performed at the operation conditions of case 1. The search for optimal values considered different stating points. Some of these points did not converge to a stable operation. Upper and lower search boundaries conditions for the controller parameters (FK_c, FK_d and FK_i) were [100, 100, 100] and [-100, -100 -100] respectively. Termination tolerance was set to $1e^{-6}$. Fig. 6a shows the searching paths for the fuzzy controller parameter starting at (FK_{c_1} = 1, FK_{d_1}= 1, FK_{i_1} = 1, FK_{c_2} = 10, FK_{d_2} = 1 and FK_{i_2} = 1). The optimal values after 40 iterations were FK_{c_1} = 61.5226, FK_{d_1} = -35.5124, FK_i = 43.1570, FK_{c_2} = 19.3028, FK_{d_2} = -6.8370 and FK_{i_2} = 1.5116. The minimizing evaluations of the integral square errors are shown on figs. (6b)-(6d). It is important to point out that ISE for FC2 is smaller than FC1 due to the magnitude of the involved variables. The same optimization process was done for the conventional PID controllers. Fig. 6c shows the searching paths for the conventional controller parameter starting at CK_{c_1} = 10, CK_{d_1} = 1, CK_{i_1} = 1, CK_{c_2} = -10, CK_{d_2} = 1 and CK_{i_2} = 1. The optimal values after 18 iterations were CK_{c_1} = 50.0125, CK_{d_1} = -0.2545, CK_{i_1} = 14.9175, CK_{c_2} = 60.2348, CK_{d_2} = -1.0179 and CK_{i_2} = 1.8247. The analysis of the five cases used the optimal controller parameters found with the operation conditions of case 1. The manipulated variables were limited to the following intervals: $N_r \in$[100, 600] rpm, and $F_w \in$[100, 10000] cm^3/min in order to guarantee the crystallizer operation within the metastable zone. In addition, simulations were performed using a seeded inlet stream with crystals of the same size, M_{43} =128 μm at temperature of 25 °C.

Table 5. Simulated partial derivatives values $(\partial F_w/\partial T)_{N_r}$ for known F_w and N_r values.

	N_r, **rpm**		
F_w, (ml/min)	**100**	**350**	**600**
150	-167.532	-169.780	-170.310
5050	-19370.0	-33.2820	-21075.0
9950	-57300.0	-57372.0	-58295.0

Table 6. Simulated partial derivatives values $(\partial N_r/\partial M_{43})_{F_w}$ for known F_w and N_r values.

	N_r, **rpm**		
F_w, (ml/min)	**105**	**355**	**595**
100	6.17970	13.0315	26.7158
5000	2.63105	9.30943	21.6452
10000	2.57050	9.26495	21.4052

Table 7. Simulated partial derivatives values $(\partial M_{43}/\partial F_w)_{N_r}$ for known F_w and N_r values.

	N_r, **rpm**		
F_w, (ml/min)	**100**	**350**	**600**
150	3.3560×10^{-2}	8.9540×10^{-2}	0.10210
5050	4.2774×10^{-4}	7.0300×10^{-4}	7.5147×10^{-4}
9950	1.3152×10^{-4}	2.2398×10^{-4}	2.2990×10^{-4}

Fig. 7 shows the closed-loop dynamic responses for control and manipulated variables. Set point in the mean crystal size was changed from 170 to 187 μm and crystallizer temperature changed from 25 °C to 23 °C. Both control algorithms allowed the system to reach the set point values in the analyzed time (25 minutes). The conventional PID control system increased quickly the cooling water flow rate in order to increase the supersaturation and favor crystal growth. This action reduced the crystallizer temperature and allowed crystals to grow beyond the established set point value (187 μm). The overshoot is eliminated reducing the cooling water flow rate. Besides, the conventional PID controller initially increased the agitation rate to favor mass transfer but after few minutes, agitation rate is reduced to the steady state operation condition. On the other hand, the fuzzy control system initially increased the agitation rate to favor mass transfer, but it kept the cooling water flow rate almost constant.

A comparison of the overall performance of both control algorithms showed faster responses for the conventional PID system. Fig. (7c)-(7d) show the manipulated variables control effort for both types of controllers. When step changes were introduced, conventional controllers reacted faster to correct changes. After 10 minutes, the control effort for both control schemes was similar. The ISE error for the conventional system was almost half of the ISE for the fuzzy control system. The evaluated values for ISE and IAE are shown on table 8. It is important to point out that minimizing the ISE, the control parameters are optimized in such a way that the closed-loop response reaches the desire value faster with a minimum overshoot. Fig. 8 shows the closed-loop dynamic responses when larger set point changes were introduced to the crystallizer. The mean crystal size set point changed from 170 μm to 210 μm and the crystallizer temperature set point changed from 25 °C to 21 °C. Optimal controller parameters previously found were used for this simulation. Figs. (8a)-(8b) show that the Fuzzy algorithm reacted faster than the conventional PID. In fact, the crystallizer temperature set point was not reached with the conventional PID controller in 25 minutes. Figs. (8c)-(8d) show the manipulated variables control effort for both types of controllers. Again, manipulated elements had larger control effort at the beginning, specially the agitation rate for the fuzzy control algorithm.

Table 8. ISE and IAE values for simulations with fuzzy and conventional PID control algorithms.

	ISE				IAE			
Change	**FC1**	**CC1**	**FC2**	**CC2**	**FC1**	**CC1**	**FC2**	**CC2**
170-187 mm 25-23 °C	459.18	199.96	3.42	1.8	43.23	45.53	4.42	1.97
170-210 mm 25-21 °C	2090.37	2403.04	16.82	28.34	119.32	133.57	9.83	24.92
170-187-195-178 mm 25-23 °C	1174.38	307.71	3.42	2.14	126.76	84.49	4.47	4.71
170-187 mm 25-23-22-23 °C	474.59	188.79	8.5	9.04	66.75	75.92	15.44	16.11
Disturbances	460.78	217.67	3.97	10.88	47.97	59.49	8.67	16.13

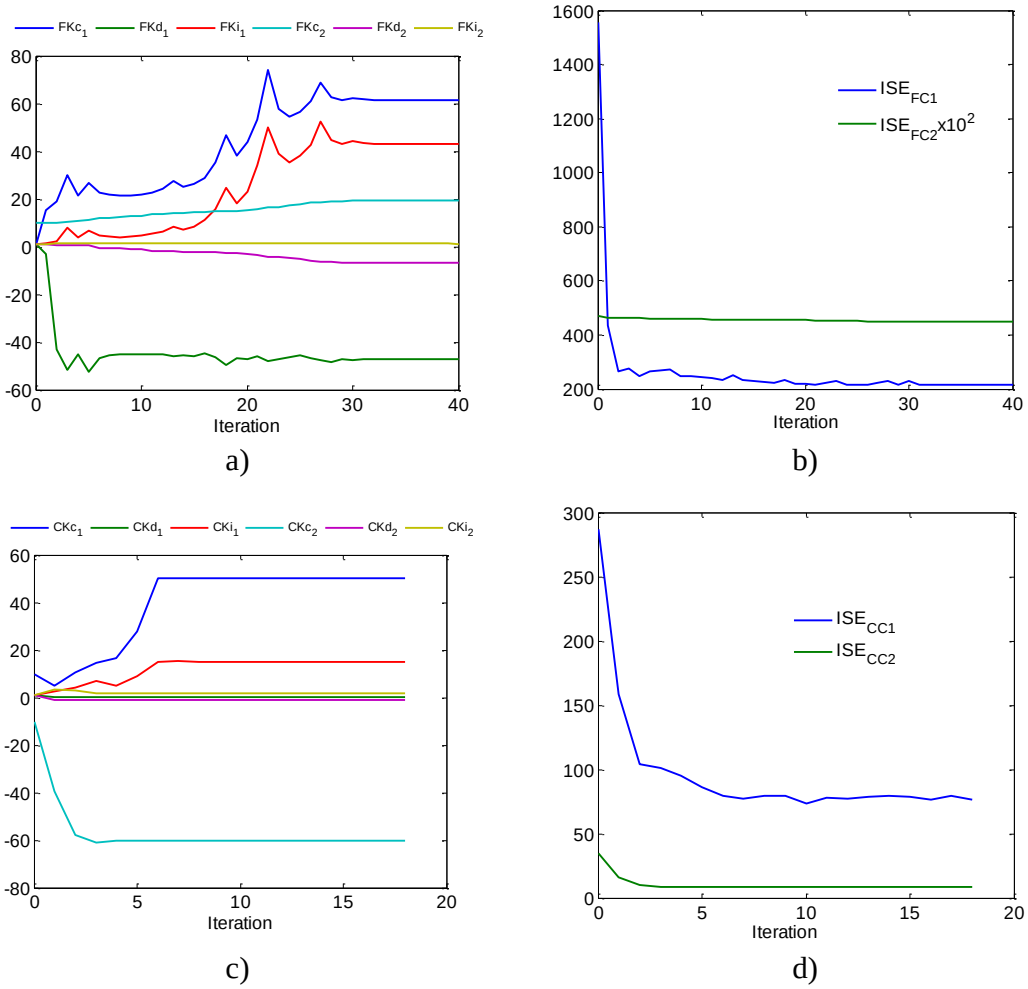

Fig. 6. Optimal searching paths of a) fuzzy controller parameters, b) integral square error for FC1 and FC2, c) conventional controller parameters and d) integral square error for CC1 and CC2.

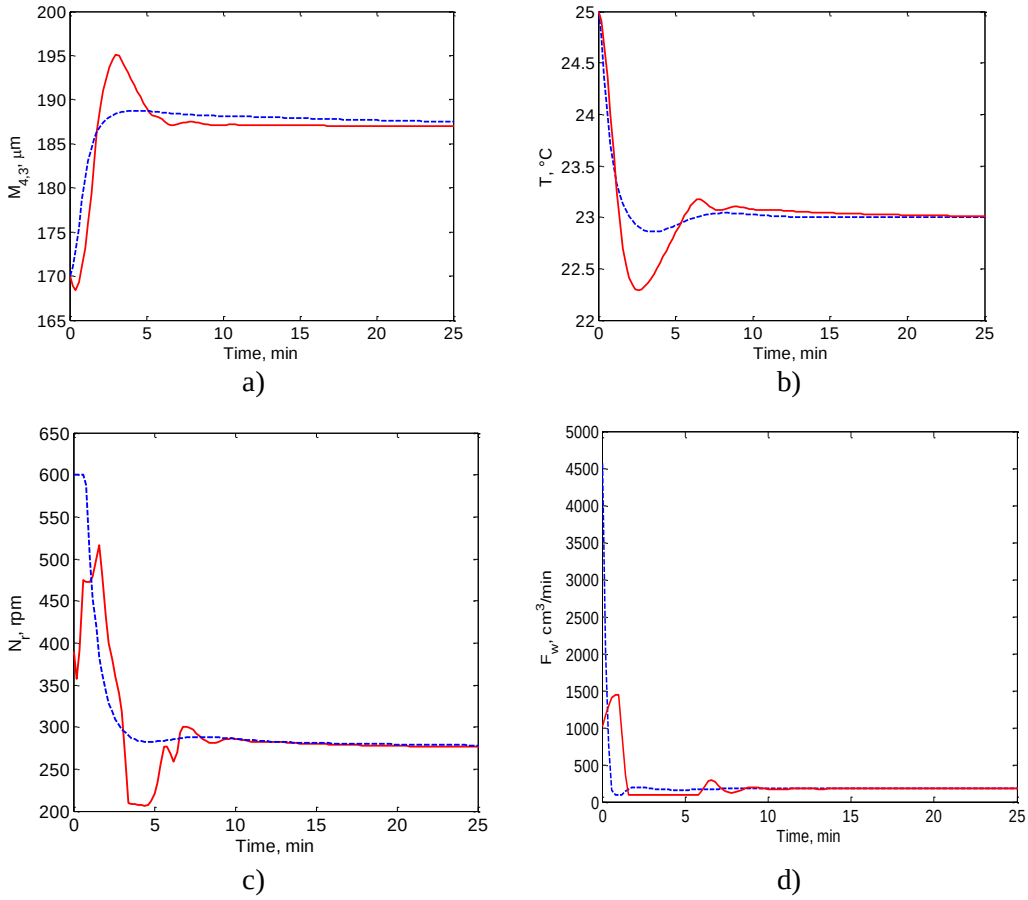

Fig. 7. Dynamic transient response of a) mean (4,3), b) temperature, c) agitation rate and d) cooling water flow rate with – – – conventional and ——— fuzzy controllers when mean (4,3) set point was increased from 170 to 187 μm and crystallizer temperature change from 25 °C to 23 °C.

After 20 minutes, there was no appreciable difference between them. In this simulation, both ISE and IAE for the fuzzy system were smaller. It would seem that the fuzzy algorithm was not as sensitive to changes in controller parameters as the conventional algorithm. Fig. 9 shows the closed-loop dynamic responses obtained for the fuzzy and conventional PID control algorithms when different set points in the mean crystal size were introduced at times 0, 25, 50 and 75 minutes. Fig. 9a shows that all set points were reached before the following set point was introduced. Fig. 9b shows a very low interaction between the control loops in the fuzzy system. It would seem that fuzzy decouplers performance was superior than conventional decouplers performance. Figs. (9c)-(9d) show the manipulated variables control effort for both types of controllers. The conventional system presented stronger demands than the fuzzy system. The low interaction between loops kept the cooling water flow rate almost constant once the crystallizer temperature steady state value was reached. The ISE for the fuzzy system was greater because it had a slower overall reaction.

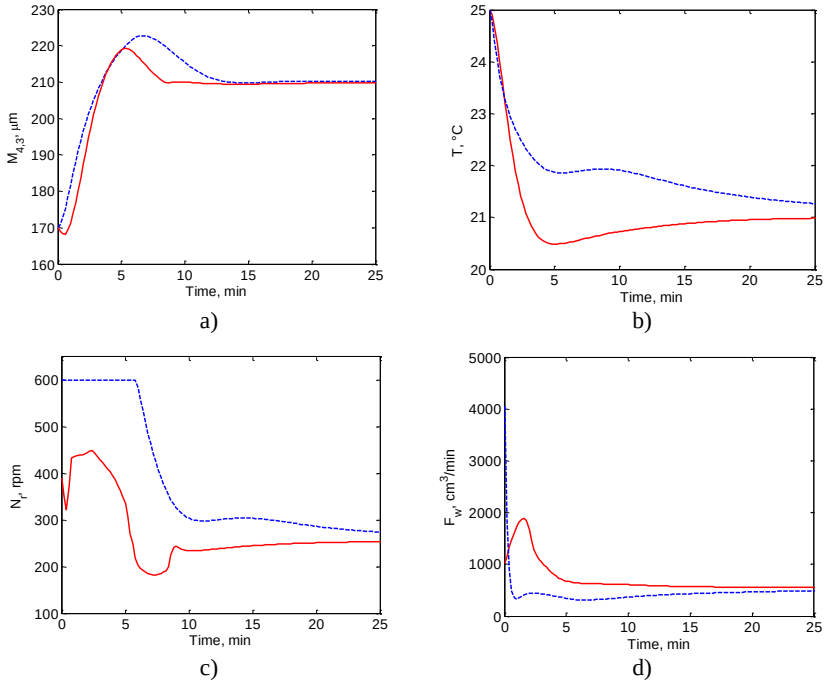

Fig. 8. Dynamic transient response of a) mean (4,3), b) temperature, c) agitation rate and d) cooling water flow rate with – – – conventional and ——— fuzzy controllers when mean (4,3) set point was increased from 170 to 210 μm and crystallizer temperature change from 25 °C to 21 °C.

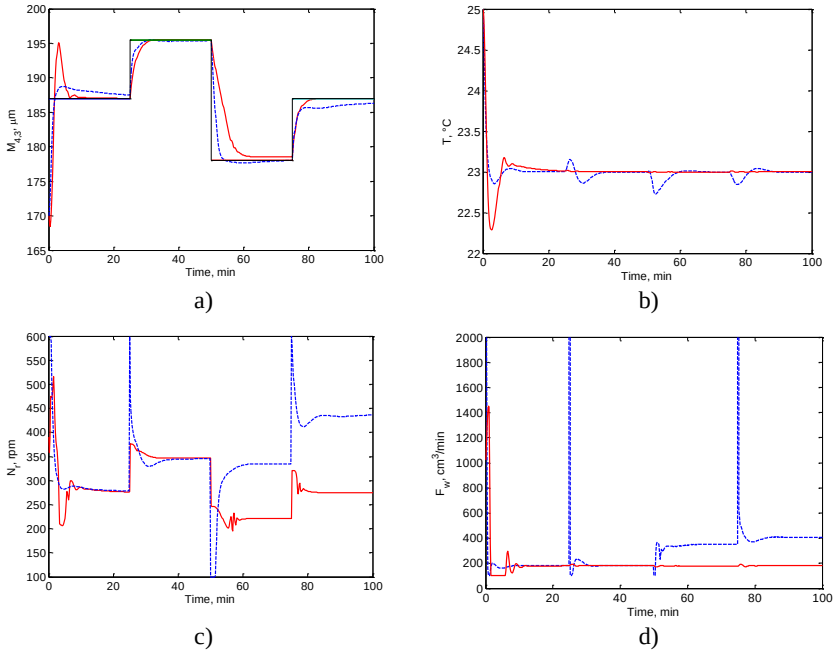

Fig. 9. Dynamic transient response of a) mean (4,3), b) temperature, c) agitation rate and d) cooling water flow rate with – – – conventional and ——— fuzzy controllers when different set point in the mean crystal size were introduced at 0, 25, 50 and 75 minutes.

The fourth analyzed case was done with changes at 0, 25, 50 and 75 minutes in the crystallizer operation temperature. Fig. 10 shows the closed-loop dynamic responses with smaller interaction between loops for the fuzzy system. The fuzzy algorithm kept the mean crystal size almost constant with manipulations in the agitation rate between 180 y 500 rpm. On the other hand, the changes in the crystallizer temperature required a stronger control effort for the F_w variable. In general, the crystallizer temperature set point changes were adequately controlled for both systems manipulating agitation rate and cooling flow rate within the established limits. The IAE´s of the fuzzy system were smaller than those of the conventional system. A comparison of the ISE for both systems showed larger values for FC1 and for CC2. The fuzzy control system had a better performance for controlling changes in the crystallizer temperatures.

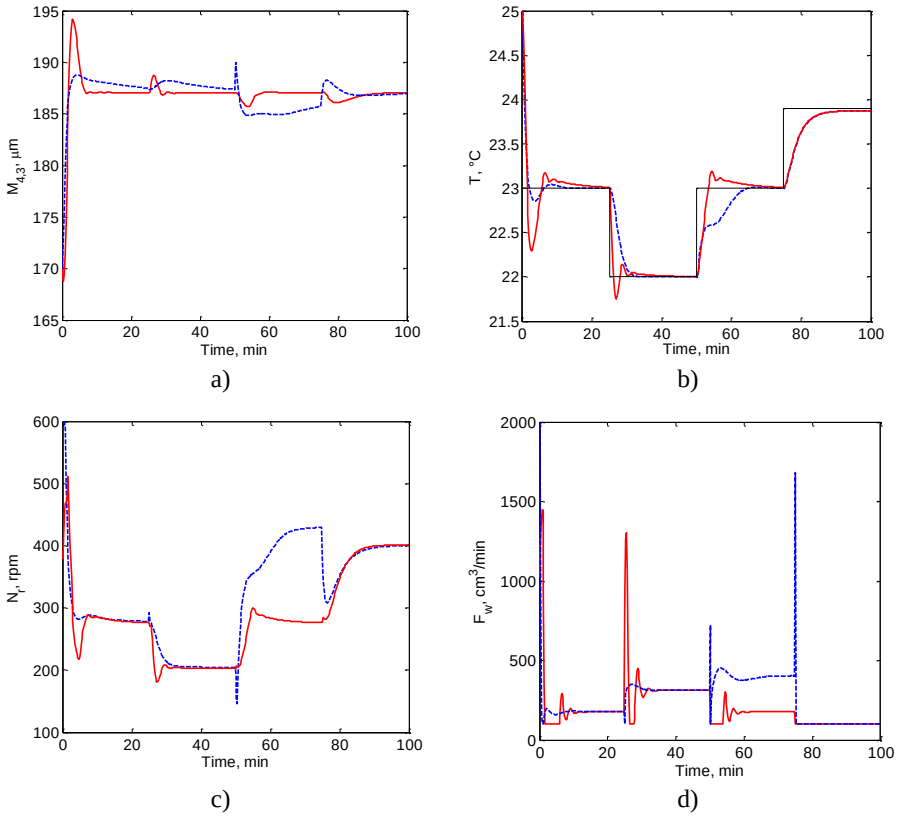

Fig. 10. Dynamic transient response of a) mean (4,3), b) temperature, c) agitation rate and d) cooling water flow rate with – – – conventional and ——— fuzzy controllers when different set point in crystallizer temperature were introduced at 0, 25, 50 and 75 minutes.

Finally, the effects of disturbances in the inlet cooling water temperature were analyzed. A change from 5 °C to 15 °C was introduced at a time 25 minutes. A second change from 15°C to 5 °C was introduced at time 50 minutes. Fig. 11 shows small effects of the disturbance on the mean crystal size but larger effects on the crystallizer temperature, especially for the conventional system. When the cooling water entered at a higher temperature, both algorithms increased the cooling water flow rate. Control effort was stronger for the conventional system due to larger controlled variables deviation. The ISE for FC1 was larger than CC1 due to the initial deviation of M_{43} but all other ISE and IAE were smaller for the fuzzy system.

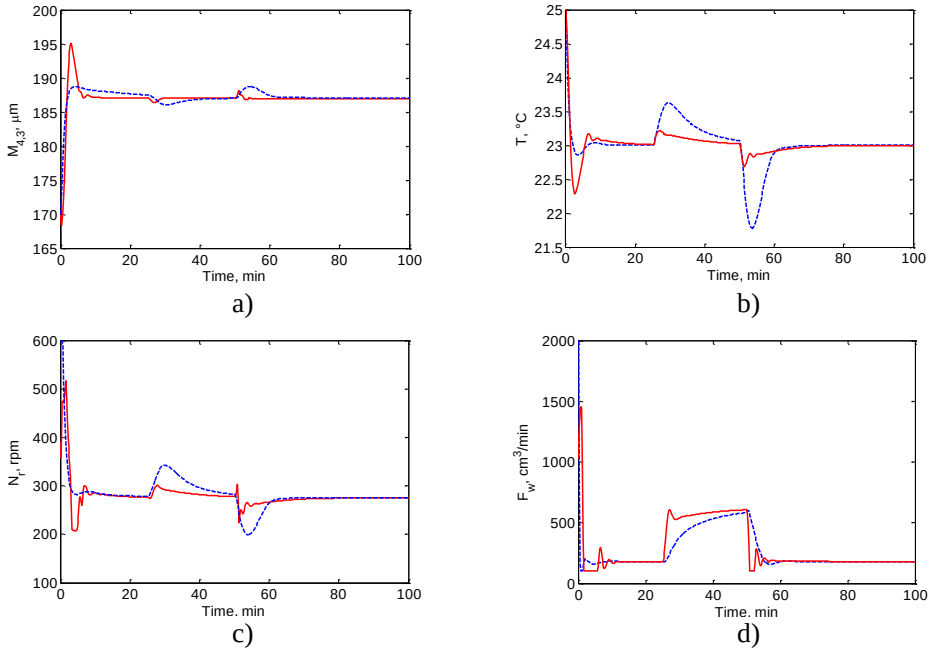

Fig. 11. Dynamic transient response of a) mean (4,3), b) temperature, c) agitation rate and d) cooling water flow rate with – – – conventional and ——— fuzzy controllers when different cooling water temperature disturbances were introduced at 0, 25 and 50 minutes.

Conclusions

Both fuzzy and conventional PID control algorithms can be successfully used to control a non-isothermal continuous crystallizer. They were able to keep the crystallizer operation stable and properly react to set point changes as well as eliminate temperature cooling disturbances effects. Conventional control systems had higher performance when used optimal controller parameters calculated at each specific operation conditions. Fuzzy control algorithms had a better performance when simulations were done with larger set point values. Finally, the fuzzy algorithm could adequately eliminate the cooling water temperature disturbance effects.

Acknowledgements

The authors want to thank DGEST (Project 2600.09) for the financial support and CONACyT Mexico for scholarships of two authors (CGAM and STA).

Nomenclature

b	nucleation equation exponent
e	controlled variable error, °C, μm
f	solution feed flow rate, cm^{3}min^{-1}
g	growing equation exponent
h	growing equation exponent
j	index
k_b	nucleation rate constant, # crystals cm^{-3}min^{-1} g^{-o} rpm^{-p}
k_g	growing rate constant, (cm^3)$^{g+1}$min^{h-1}g^{-g}rpm^{-h}
k_v	shape factor
o	nucleation equation exponent
p	nucleation equation exponent
u	control action, cm^3 min^{-1}; rpm
B	nucleation rate, # crystals cm^{-3}min^{-1}
C	solute concentration, gcm^{-3}
C_l	meta stable limit concentration, gcm^{-3}
C_s	saturation concentration, gcm^{-3}
C_p	solution heat capacity, cal g^{-1} C^{-1}
C_{pw}	water heat capacity, cal g^{-1} °C^{-1}
F_w	water cooling flow rate, cm^3 min^{-1}
G	growing rate, cm min^{-1}
K	weight constant
CK_c	conventional controller proportional gain
CK_d	conventional controller derivative gain
CK_i	conventional controller integral gain
FK_C	fuzzy controller proportional gain
FK_d	fuzzy controller derivative gain

FK_i	fuzzy controller integral gain
M_{43}	crystal size distribution mean (M_4/M_3), μm
M_j	j-th crystal size distribution moment, # crystals cm^{-3+j}
M_t	crystal total mass, g
N_r	agitation rate, rpm
S_r	relative supersaturation
T	solution temperature, °C
T_c	jacket temperature, °C
T_∞	environment temperature, °C
UA	heat transfer rate (crystallizer-jacket), cal min^{-1} °C^{-1}
UA_∞	heat transfer rate (jacket-environment), cal min^{-1} °C^{-1}
V	crystallizer volume, cm^3
V_c	jacket volume, cm^3

Greek symbols

ε	solid free fraction
ρ	solution density, g cm^{-3}
ρ_c	crystal density, g cm^{-3}
ρ_w	water density, g cm^{-3}
τ	residence time, min
ΔH_c	crystallization enthalphy, cal g^{-1}

References

Andújar, J.M., and Bravo, J.M. (2005). Multivariable fuzzy control applied to the physical-chemical treatment facility of a cellulose factory. *Fuzzy Sets and Systems 150*, 475-492.

Bravi, M., and Chianese, A. (2003). Neuro-fuzzy control of a continuous cooled MSMPR crystallizer. *Chemical Engineering Technology 26*, 262-266.

Chebolu, S. (2004). *Fuzzy control of a rotatory inverted pendulum swing-up using Matlab and Simulink*. M.S. Thesis, Texas A&M University-Kingsville, USA.

Chen, J.Y., and Chang, C.T. (2006). Fuzzy diagnosis method for control systems with coupled feed forward and feedback loops. *Chemical Engineering Science 61*, 3105-3128.

Gupta, D. (2005). *Controlling the velocity and azimuth of a mobile robot using fuzzy logic*. M.S. Thesis, Texas A&M University-Kingsville, USA.

Kim, J.H., and Oh, S.J. (2000). A fuzzy PID controller for nonlinear and uncertain systems.

Soft Computing 4, 123-129.

Kocaarslan, Ì., Çam, E., and Tiryaki, H. (2006). A fuzzy logic controller application for thermal power plants. *Energy Conversion and Management 47*, 442-458.

Lakatos,B.G., Sapundzhiev, T.J., and Garcide, J. (2007). Stability and dynamics of isothermal CMSMPR crystallizers. *Chemical Engineering Science 62*, 4348-4364.

Li, C., and Priemer, R. (1999). Fuzzy control of unknown multiple-input-multiple-output plants. *Fuzzy Sets and Systems 104*, 245-267.

Lian, R.J., and Huang, S.J. (2001). A mixed fuzzy controller for MIMO systems. *Fuzzy Sets and Systems 120*, 73-93.

Lugo, J.R. (2005). *Estudio para la determinación de la zona metaestable a través del análisis del proceso de nucleación para el sulfato de amonio*. M.S. Thesis, Instituto Tecnológico de Celaya, México.

Odetunji, O.A., and Kehinde, O.O. (2005). Computer simulation of fuzzy control system for gari fermentation plant. *Journal of Food Engineering 68*, 197-207.

Park, Y., and Cho, H. (2005). A fuzzy logic controller for the molten steel level control of strip casting processes. *Control Engineering Practice 13*, 821-834.

Pathath, P.K., and Kienle, A. (2003)A numerical bifurcation analysis of nonlinear oscillations in crystallization processes. *Chemical Engineering Science 57*, 4391-4399.

Perry, R.H., Green, D.W., and Maloney, J.O. (1992). *Chemical Engineering Handbook. McGraw Hill Ed*.

Quintana-Hernandez, P.A., Moncada-Abaunza, D.A., Bolaños-Reynoso, E., and Salcedo-Estrada, L.I. (2005). Evaluación del crecimiento de cristales de azúcar y determinación del factor de forma de área superficial. *Revista Mexicana de Ingeniería Química 4(1)*, 123-129.

Quintana-Hernández, P.A., Ocampo-Pérez, R., Tututi-Ávila, S., and Hernández-Castro, S. (2012). Nonlinear MIMO control of a continuous cooling crystallizer. *Modellig and Simulation in Engineering 2012*, 1-11.

Quintana-Hernández, P. A., Díaz-Pérez,G., Rico-Ramírez, V., and Salcedo-Estrada, L. I. (2016). Metastable zone width measurement of adipic acid-water solutions. *Revista Mexicana de Ingeniería Química 53(1)*, 1009-1018.

Salcedo-Estrada, L.I. (2000). *Control de cristalizadores tipo batch*. Ph.D. Thesis, Instituto Tecnológico de Celaya, México.

Shaocheng, T., Bin, C., and Yongfu, W. (2005). Fuzzy adaptive output feedback control for MIMO nonlinear systems. *Fuzzy Sets and Systems 156*, 285-299.

Shelare, M. (2004). *Fuzzy Logic Controller for Steady Level Flight of F-16 Aircraft Using Matlab and Simulink*, M.S. Thesis, Texas A&M University-Kingsville, USA.

Thompson, R., and Dexter, A. (2005). A fuzzy decision-making approach to temperature control in air-conditioning systems. *Control Engineering Practice 13*, 689-698.

Tututi-Ávila, S. (2007). *Desarrollo de un algoritmo de control para el proceso de cristalización usando lógica difusa*. M.S. Thesis, Instituto Tecnológico de Celaya, México.

Zempoaltécatl, E. (2006). *Estudio para el control de la distribución del tamaño del cristal usando modelos predictivos*. M.S. Thesis, Instituto Tecnológico de Celaya, México.

Zhang, T.P., and Feng, C.B. (1997). Decentralized adaptive fuzzy control for large-scale nonlinear systems. *Fuzzy Sets and Systems 92*, 61-70.